Macromolecules **2006,** *39,* 81−89

RAFT Synthesis of a Thermally Responsive ABC Triblock Copolymer Incorporating *N*-Acryloxysuccinimide for Facile in Situ Formation of Shell Cross-Linked Micelles in Aqueous Media[†]

Yuting Li, Brad S. Lokitz, and Charles L. McCormick*

Department of Polymer Science, The University of Southern Mississippi,
Hattiesburg, Mississippi 39406-0076

Received September 29, 2005; Revised Manuscript Received November 1, 2005

ABSTRACT: A poly(ethylene oxide) (PEO)-based macromolecular chain transfer agent (macro-CTA) was employed to demonstrate the controlled polymerization of *N*,*N*-dimethylacrylamide (DMA) in anhydrous 1,4-dioxane at 70 °C using reversible addition−fragmentation chain transfer polymerization. This macro-CTA was then used to mediate the statistical copolymerization of DMA and the reactive monomer *N*-acryloxysuccinimide (NAS), forming a diblock copolymer of PEO-*b*-(DMA-*s*-NAS). Subsequent chain extension with *N*-isopropylacrylamide (NIPAM) yielded a PEO-*b*-(DMA-*s*-NAS)-*b*-NIPAM thermally responsive triblock copolymer. In aqueous solution at room temperature the triblock copolymer chains exist as unimers but form micelles when the solution temperature is raised above the lower critical solution temperature (LCST) of the NIPAM block. The hydrodynamic dimensions and micellization temperatures depend on the length of the NIPAM block. Incorporation of the NAS units into the triblock copolymer allows for facile formation of uniform shell cross-linked micelles by reaction with difunctional primary amines in aqueous media. These shell cross-linked micelles swell when the solution temperature is lower than the LCST of the NIPAM block.

Introduction

Shell cross-linked (SCL) micelles were first reported by Wooley and co-workers in 1996.[1] Since then, SCL micelles have attracted much attention because they combine the properties of micelles, microgels, nanoparticles, and dendrimers. Potential applications include targeted drug delivery, emulsification, sequestration of metabolites, and entrapment of environmental pollutants.[2−12]

The preparation of SCL micelles from AB diblock copolymers is usually carried out at very dilute solutions (typically $<$0.50% solids) in order to avoid extensive intermicellar cross-linking. Recently, Armes and co-workers[13,14] reported that ABC triblock copolymers offer great advantages over conventional AB diblock copolymers since the former allow for shell cross-linking at high solids (10%) with little or no intermicellar cross-linking.

To date, several methods have been employed for shell cross-linking. 1,2-Bis(2-iodoethoxy)ethane has been used by Armes and co-workers to cross-link 2-(dimethylamino)ethyl methacrylate residues via quaternization.[14−17] Wooley's group has reported carbodiimide coupling chemistry to link carboxylic acid groups via diamines.[18,19] Liu et al. utilized divinyl sulfone to successfully cross-link hydroxylated blocks.[20] Other cross-linking methods including UV-induced coupling[21] and ionically induced polyelectrolyte complexation[22] have also been reported. However, it is recognized that more facile techniques would be desirable since all of the above-mentioned cross-linking methods have their own limitations.[20,22]

The synthesis of well-defined diblock or triblock copolymers requires that a controlled/"living" polymerization technique be employed. Controlled/"living" radical polymerization methods including nitroxide-mediated polymerization,[23] atom transfer radical polymerization (ATRP),[24] and reversible addition−fragmentation chain transfer (RAFT)[25] polymerization are effective for preparing complex architectures such as blocks and stars.[24,26−29] Although each controlled/"living" radical polymerization technique has its own characteristics and advantages, RAFT is arguably the most versatile since it is compatible with most functional monomers under conditions that are similar to conventional free radical polymerization.[27,30]

Our group has a long-standing interest in the RAFT polymerization and copolymerization of hydrophilic acrylamido monomers[31] including anionic,[32,33] cationic,[34] zwitterionic,[35,36] and neutral derivatives.[37−39] Herein, we report the successful RAFT copolymerization of *N*,*N*-dimethylacrylamide (DMA) with *N*-acryloxysuccinimide (NAS) using a poly(ethylene oxide) methyl ester (PEO)-based macro-chain transfer agent (macro-CTA). The resulting diblock copolymer macro-CTA was then used for the polymerization of *N*-isopropylacrylamide (NIPAM), creating a PEO-*b*-(DMA-*s*-NAS)-*b*-NIPAM triblock copolymer. In aqueous solution, this triblock copolymer self-assembles to form NIPAM-core micelles when the solution temperature is raised above the lower critical solution temperature (LCST) of the NIPAM block. These micelles can be shell cross-linked using difunctional primary amines such as ethylenediamine. Although shell cross-linked micelles have been reported by several authors,[1,15,21] to the best of our knowledge, this is the first time that NAS has been used to provide a cross-linkable functional group. Obviously, the advantage of our current method is that any monomer, as long as it can copolymerize with NAS, can be used as the shell block of the micelles. This procedure will expand the currently limited number of monomer choices used for SCL micelles.

Experimental Section

Materials. DMA (99%, Aldrich) was dried over calcium hydride, vacuum-distilled, and purged with nitrogen prior to use. NIPAM (97%, Aldrich) was recrystallized twice from a benzene/hexane mixture. 2,2-Azobis(isobutyronitrile) (AIBN, 98%, Fluka) was recrystallized twice from ethanol. Carbon disulfide (99.9+%, HPLC

[†] Paper number 115 in a series on Water-Soluble Polymers.

* To whom correspondence should be addressed. E-mail: Charles.McCormick@usm.edu.

10.1021/ma052116r CCC: \$33.50

grade,), magnesium turnings (>99.5%), 2-chloro-2-phenylacetyl chloride (CPAC, 90%), poly(ethylene oxide) methyl ester (PEO) ($M_n = 2000$ g mol^{-1}, $M_w/M_n = 1.10$), diethyl ether, ethyl acetate, and *n*-hexane were purchased from Aldrich (AR grade) and used as received. All other chemicals were purchased from Fisher or Aldrich at the highest available purity and used as received.

***N*-Acryloxysuccinimide.** NAS monomer was synthesized according to a literature procedure[40] by direct esterification of the *N*-hydroxysuccinimide (NHS) with acryloyl chloride in the presence of triethylamine (TEA).

Esterification of PEO with Chlorophenylacetic Acid.[43] Poly(ethylene oxide) methyl ester (20.0 g, 10.0 mmol), TEA (4.2 mL, 30 mmol), and 2-chloro-2-phenylacetyl chloride (3.0 mL, 20 mmol) were mixed in a round-bottom flask using dry tetrahydrofuran (THF) (200 mL) as solvent, and the solution was refluxed for 2 days at atmospheric pressure. The solvent was then removed, and chloroform (150 mL) was added. The resulting solution was washed with saturated sodium bicarbonate solution, and the yellow organic phase was dried over anhydrous magnesium sulfate. The solvent was then removed in vacuo to give an ester of chlorophenylacetic acid with poly(ethylene oxide) methyl ester (PEO−CPA). The product (95%) was further purified by precipitation in cold diethyl ether. ^{1}H NMR ($CDCl_3$, 298 K, 200 MHz), δ (ppm from TMS): 3.36 (3H, s, O−C*H*$_3$), 3.60 (4H, s, C*H*$_2$−C*H*$_2$−O), 5.39 (1H, s, C*H*Cl), 7.36 (5H, m, Ar−*H*).

Synthesis of PEO Macro-CTA.[43] A THF solution (10 mL) of 4-fluorobromobenzene (2.2 mL, 20 mmol) was added dropwise to a mixture of Mg (0.50 g, 20 mmol) in THF (40 mL) and a crystal of I_2 in a two-necked round-bottom flask equipped with a condenser and a magnetic stirrer with a nitrogen atmosphere. The mixture was refluxed for 4 h and then cooled to room temperature. Carbon disulfide (4.0 mL, 66 mmol) was added dropwise, and the solution was stirred for 1 h. This solution was then added to the PEO−CPA solution (10.0 g in 40 mL of THF) and refluxed overnight. The orange-red product was precipitated in cold diethyl ether to give PEO−CTA (10.0 g, 98%). ^{1}H NMR ($CDCl_3$, 298 K, 200 MHz), δ (ppm from TMS): 3.33 (3H, s, O−C*H*$_3$), 3.63 (4H, m per C*H*$_2$−C*H*$_2$−O), 5.69 (1H, s, −SC*H*(Ph)−CO$_2$), 7.0−8.1 (9H, m, Ar−*H*).

Synthesis of the PEO-*b*-(DMA-*s*-NAS) Diblock Copolymers. DMA (2.38 g, 24 mmol), NAS (1.01 g, 6.0 mmol), PEO−CTA (0.69 g, 0.30 mmol), and AIBN (9.8 mg, 0.060 mmol) were added along with 1,4-dioxane (4.5 mL) to an ampule. The ampule was sparged with nitrogen for ∼30 min and then placed in a preheated oil bath at 70 °C. The reaction was terminated after 24 h by cooling the reaction tube in an ice bath followed by exposure to air. The PEO-*b*-(DMA-*s*-NAS) diblock copolymer was then precipitated in cold diethyl ether (conversion = 73%, $M_n = 15\,500$, and PDI = 1.11). To determine the NAS content in the PEO-*b*-(DMA-*s*-NAS) diblock copolymers, 5.0 mg of PEO-*b*-(DMA-*s*-NAS) diblock copolymer was dissolved in 1.0 mL of D_2O; benzylamine (20.0 mg) was then added. After 30 min, the solution was examined by ^{1}H NMR to determine the NAS content by comparing the peak integration area of PEO methylene proton at 3.5 ppm to that of NHS proton at 2.45 ppm. Calculation of the number of NAS and DMA repeating units from conversion, NMR, and molecular weight data allow us to determine the statistical block composition. For example, the PEO-(DMA-*s*-NAS) copolymer in this example is designated as PEO$_{45}$-*b*-(DMA$_{92}$-*s*-NAS$_{31}$). Block lengths are so designated throughout the text.

Synthesis of the PEO-*b*-(DMA-*s*-NAS)-NIPAM Triblock Copolymers. NIPAM (0.35 g, 3.1 mmol), PEO$_{45}$-*b*-(DMA$_{92}$-*s*-NAS$_{31}$) (0.40 g, 0.026 mmol), and AIBN (0.85 mg, 0.005 mmol) were added along with 1,4-dioxane (2.0 mL) to an ampule. After purging with nitrogen for 30 min, the reaction was allowed to proceed at 70 °C for 16 h. The reaction was quenched by cooling the reaction vessel in an ice bath and the solution subsequently exposed to air. The triblock copolymer was precipitated in cold diethyl ether (conversion = 74%, $M_n = 28\,600$, and PDI = 1.23.)

Preparation of Micelles and Shell Cross-Linked Micelles. The PEO$_{45}$-*b*-(DMA$_{92}$-*s*-NAS$_{31}$)-*b*-NIPAM$_{91}$ triblock copolymers (30 mg) were dissolved in D_2O (3.0 mL) at room temperature, and the solution was filtered through a 0.02 μm filter. A 10 mL vial containing 2.0 mL of this solution was suspended in a 44 °C water bath. The solution was equilibrated for 30 min to allow the formation of uniform micelles. At the same time, a solution of ethylenediamine (1.0 mg) in 3.0 mL of D_2O was placed in the water bath at 44 °C and allowed to equilibrate for 30 min. Then 2.0 mL of the ethylenediamine solution was added to the triblock copolymer solution. The final copolymer concentration was 5 g/L, and the ethylenediamine/NAS molar ratio was kept at 1:2. The solution was stirred for 16 h at 44 °C.

Characterization. The molecular weights of the copolymers were determined using Viscotek-TDA (302 RI (633 nm), 7 mW 90° and 7° true low-angle light scattering detectors, $\lambda = 670$ nm) size exclusion chromatography (SEC) equipped with two Polymer Labs PLgel 5 μm (30 cm) Mixed "C" columns (200−2 000 000 g/mol) at 60 °C. The mobile phase consisted of HPLC grade DMF. The flow rate was maintained at 0.5 mL min^{-1} using an Agilent 1100 series pump. The molecular weight and polydispersity data were determined using the OmniSEC software package (version 2,0,2,89) based on d*n*/d*c* = 0.081. Near-monodisperse linear poly(2-vinylpyridine) standards (purchased from Scientific Polymer Products, Inc.) were used to construct the calibration curve. ^{1}H NMR spectra were recorded in D_2O or $CDCl_3$ using a Varian Mercury 200 MHz spectrometer. Spectra at temperatures other than room temperature were recorded using a temperature-controlled Mercury Innova 500 MHz spectrometer. Dynamic light scattering studies of the block copolymer micelles in aqueous solution were conducted using Malvern Instruments Zetasizer Nano Series instrument equipped with a 22 mW He−Ne laser operating at $\lambda = 632.8$ nm, an avalanche photodiode detector with high quantum efficiency, and an ALV/LSE-5003 multiple tau digital correlator electronics system. Atomic force microscopy (AFM) images were collected in tapping mode using standard RTESP silicon cantilever (length: 125 μm; spring constant: 20−80 N/m; and resonance frequency: about 300 kHz) (VEECO Probes, CA) in Dimension 3000 scanning probe microscope (Digital Instruments). The sizes of the micelles were obtained by section analysis using Nanoscope version 5.30 r2 software.

Results and Discussion

PEO-Based Macro-CTA. PEO was chosen as the first segment of our ABC triblock based on its recognized biocompatibility and solubility in both aqueous and organic media. Additionally, there is literature precedence for block formation from PEO-based ATRP macroinitiators[20,41] and PEO-based macro-CTA's.[42,43] We have chosen a method similar to that reported by Perrier and co-workers to prepare dithioester RAFT agent.[43] This facile procedure outlined in Scheme 1 yielded our methoxy-terminated PEO$_{45}$ macro-CTA in which the *p*-fluoro dithioester (Z group) would be expected to raise the ground-state reactivity of the C═S double bond toward radical addition while sufficiently stabilizing the intermediate radical.[44−46] Additionally, the substituted R group is expected to be a sufficiently good leaving group and reactive enough for addition to DMA for efficient blocking.[44,47−49]

PEO-*b*-DMA Copolymers. RAFT polymerization of DMA in both organic and aqueous solvents has been the subject of extensive research in our group and others.[37,44,50,51] Utilizing AIBN and 1,4-dioxane as the initiator and solvent, respectively, DMA polymerized in a facile manner at 70 °C with our PEO macro-CTA. Our attempts to conduct the polymerization at 60 °C were not successful due to unacceptably slow conversions. Aliquots obtained over the course of the reaction were utilized to (a) examine the evolution of molecular weight and molecular weight distribution with conversion and (b) monitor the kinetic profile based on monomer conversion vs time.

Scheme 1. Synthetic Pathway for Formation of the Poly(ethylene oxide)-Based Macromolecular Chain Transfer Agent

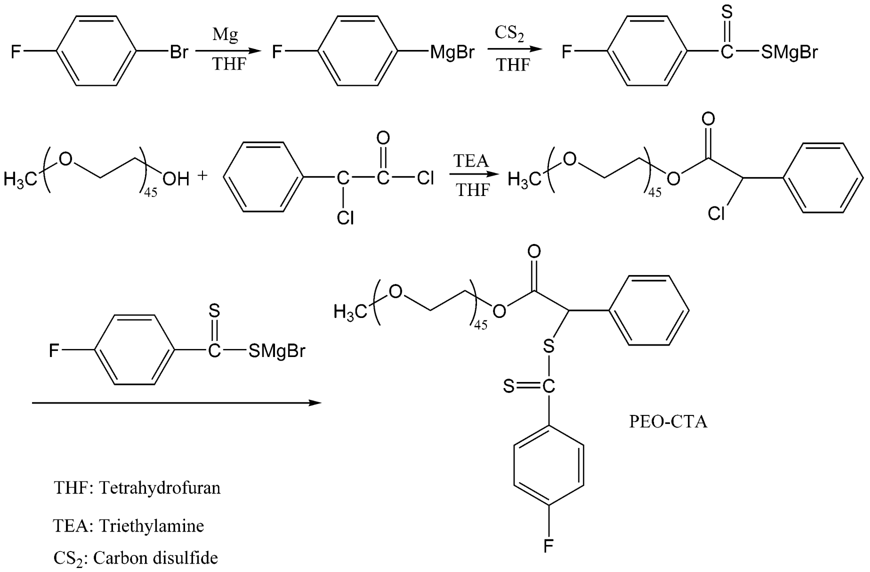

Table 1. Evolution of the Molecular Weights and Polydispersities during the RAFT Polymerization of DMA with PEO$_{45}$ Macro-CTA at 70 °C in Dioxane[a]

entry no.	time (h)	conv (%)	M_n	M_w	M_w/M_n
1	1	0	2300	2500	1.10
2	2	4	2600	2900	1.09
3	4	26	4300	5500	1.29
4	5	35	5500	7100	1.29
5	6.5	48	6700	9200	1.37
6	8.5	58	7100	11300	1.58
7	12	70	8100	13600	1.68
8	18	79	9400	16000	1.71
9	24	85	9800	17500	1.78
after purification			15900	18500	1.17

[a] Conditions: 0.458 g (0.2 mmol) of PEO$_{45}$-CTA; 1.98 g (20 mmol) of DMA; 0.00656 g (0.04 mmol) of AIBN; 3.0 mL of dioxane. dn/dc = 0.081 was used to calculate the polymer molecular weight and molecular weight distribution.

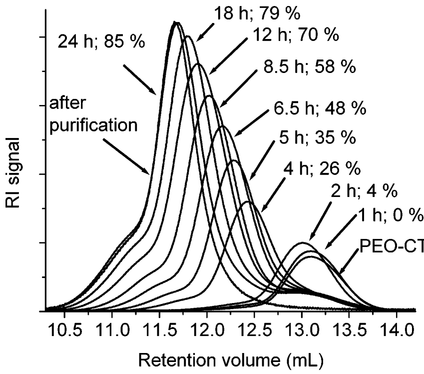

Figure 1. SEC chromatograms (refractive index detector, RI) obtained after selected polymerization times during the reversible addition–fragmentation chain transfer polymerization of PEO$_{45}$-*b*-DMA$_{100}$ in 1,4-dioxane at 70 °C. See Table 1 for detailed conditions. PEO = poly(ethylene oxide); DMA = *N*,*N*-dimethylacrylamide.

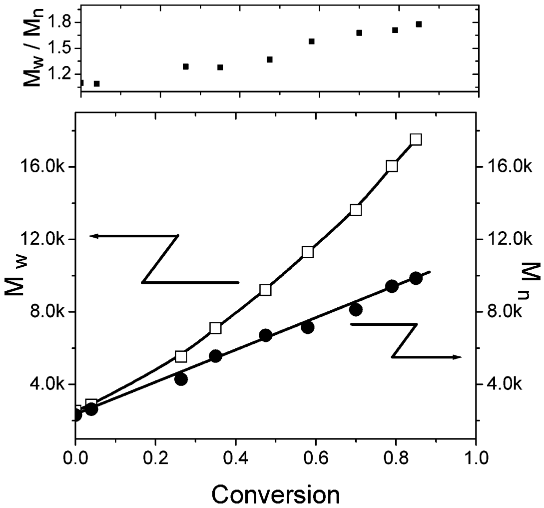

Figure 2. Evolution of weight-average (M_w) and number-average (M_n) molecular weights and M_w/M_n values with conversion for the homopolymerization of *N*,*N*-dimethylacrylamide with poly(ethylene oxide)-based macromolecular chain transfer agent in 1,4-dioxane at 70 °C. See Table 1 for detailed conditions.

Figure 1 and Table 1 show the block copolymer molecular weight vs time data. Throughout the reaction, a shoulder at low retention volume is present which has been attributed to bimolecular coupling in other studies of DMA polymerization with phenyl Z groups and/or less reactive reinitiating R groups.[37,44] Also evident at higher retention volume is a residual signal from the PEO macro-CTA, indicating less than 100% dithioester functionalization. The chain transfer efficiency appears to be ~70%, and the unreactive PEO is also responsible for some of the M_w/M_n broadening with conversion (Figure 2). Fortunately, the unreacted PEO homopolymer is easily removed by precipitating the block copolymer in diethyl ether, as can be readily seen by comparison of Figure 1 chromatograms of the purified sample and the reaction aliquot (last entry and ninth entry, respectively, in Table 1). After purification, which also readily removes unreacted DMA, the M_w/M_n value of the block is 1.17 at a conversion of 85%. From a practical experimental viewpoint, the unfunctionalized PEO is not detrimental to successful preparation of the PEO-*b*-DMA macro-CTA, and it is easily removed prior to or after blocking or chain extension.

The first-order kinetic plot (Figure 3) is linear up to 60% conversion (~10 h). Beyond this point (exceeding the half-life of AIBN at 70 °C), behavior becomes increasingly nonlinear. Primary radical coupling and the lack of AIBN-generated radicals for CTA activation contribute to this nonlinearity.

PEO-*b*-(DMA-*s*-NAS) Copolymers. Having established a suitable polymerization procedure for the homopolymerization of DMA from the PEO macro-CTA, we then examined the incorporation of an active monomer by the statistical copolymerization of DMA with NAS. NAS was chosen as the active

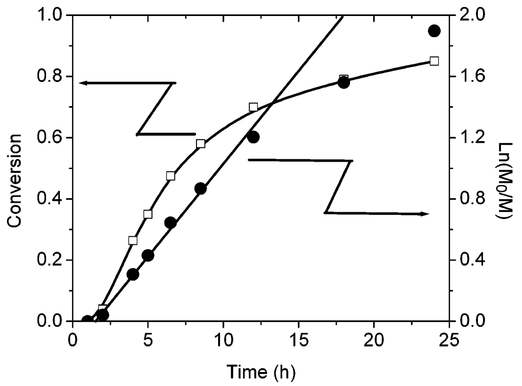

Figure 3. Fractional conversion and $\ln(M_0/M)$ vs time plots for the polymerization of *N*,*N*-dimethylacrylamide with the poly(ethylene oxide)-based macromolecular chain transfer agent in 1,4-dioxane at 70 °C. See Table 1 for detailed conditions.

monomer due to its enhanced activity toward primary amines and relatively lower susceptibility to hydrolysis.[52] The copolymerization of NAS with other vinyl monomers via RAFT has already been reported[52,53] although the homopolymerization of NAS by RAFT is uncontrolled.[54] Such polymer precursors have been used as supports for oligonucleotide synthesis, to elaborate polymer−oligonucleotide conjugates,[55] or used as active sites in the synthesis of comblike polymers.[56] Our results for the RAFT copolymerization of DMA with NAS in 1,4-dioxane (Scheme 2) are listed in Table 2. The polydispersities of the copolymers are relatively narrow (<1.2), indicating good control of the polymerization. Figure 4 shows the ^{1}H NMR spectra of the PEO macro-CTA and PEO-*b*-(DMA-*s*-NAS) copolymers. Spectral overlap between the four methylene protons on NAS with the six methyl protons on DMA makes it impractical to accurately calculate the NAS content of the diblock copolymers directly. To obtain the copolymer compositions, the NAS moieties were reacted with excess amounts of benzylamine. By comparing the resonance associated with the PEO units to those of the NHS byproduct (δ 2.4, ^{1}H NMR spectrum not shown), the NAS content in the copolymer was calculated (Table 2).

PEO-*b*-(DMA-*s*-NAS)-*b*-NIPAM Triblock Copolymers. NIPAM is an extensively studied nonionic, acrylamido monomer since its homopolymer (PNIPAM) possesses a readily accessible LCST of ~32 °C in aqueous solution, close to human body temperature (37 °C). For this reason, PNIPAM has been evaluated in drug delivery applications.[57−59] Several groups have already reported the successful RAFT polymerization of NIPAM.[60−63] We used PNIPAM as the third block in our ABC triblock copolymers. The ABC triblock copolymer was synthesized using the PEO$_{45}$-*b*-(DMA-*s*-NAS) as the macro-CTA in

Scheme 2. (a) Reaction Pathway for the Synthesis of the PEO-*b*-(DMA-*s*-NAS)-*b*-NIPAM Triblock Copolymers; (b) Illustration of the Formation of Three-Layer Micelles and Shell Cross-Linked Micelles from PEO-*b*-(DMA-*s*-NAS)-*b*-NIPAM Triblock Copolymers

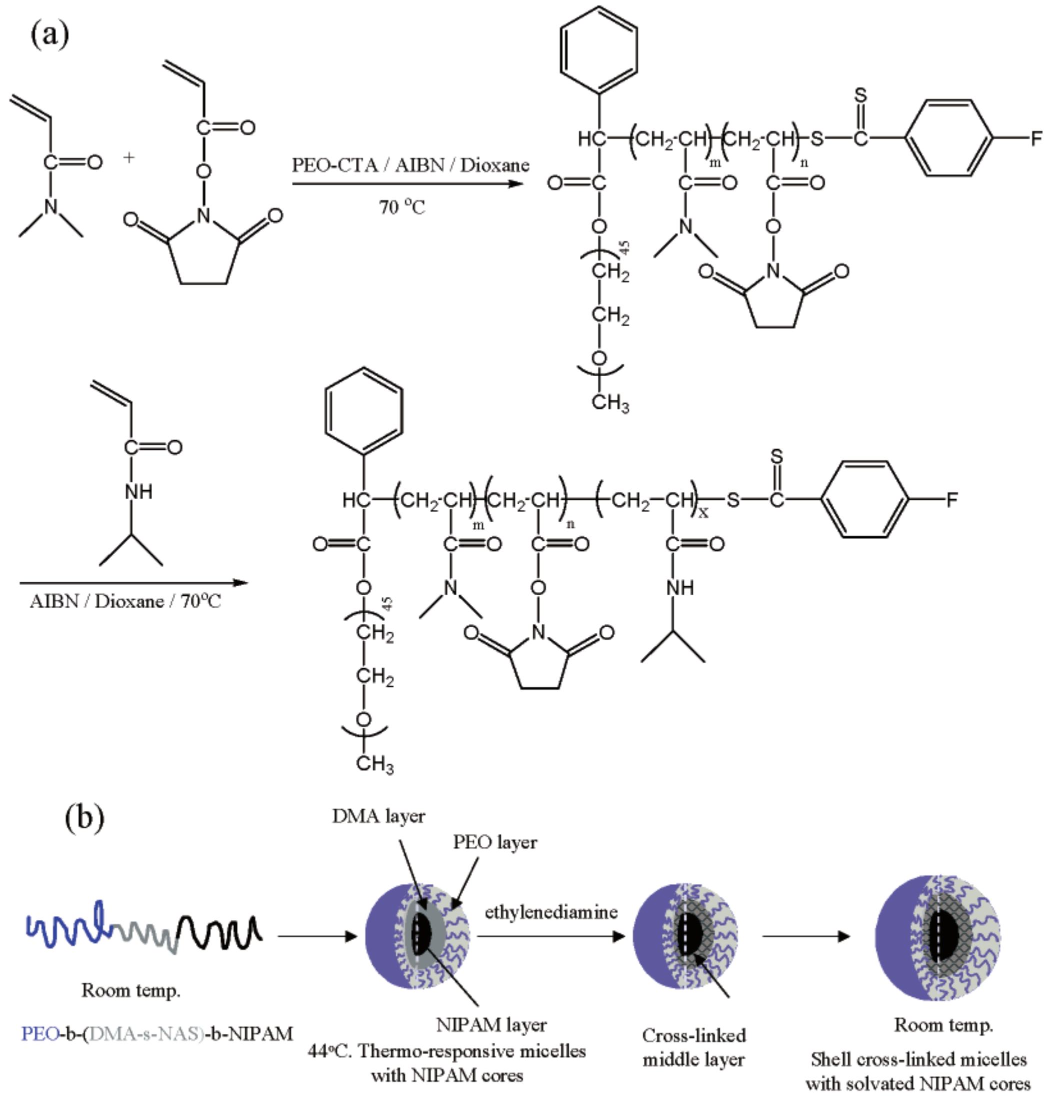

Table 2. Summary of the Reaction Conditions for the Synthesis of the Diblock and Triblock Copolymers by RAFT in 1,4-Dioxane at 70 °C with AIBN as Initiator[a]

entry no.	target copolymer structure (subscripts refer to Dp)	time (h)	conv (%)	M_n	M_w	M_w/M_n	M_n[b]	real structure[b]
1	PEO$_{45}$-*b*-(DMA$_{100}$-*s*-NAS$_{10}$)	7	67	13 100	14 800	1.13	13 200	PEO$_{45}$-*b*-(DMA$_{91}$-*s*-NAS$_{12}$)
2	PEO$_{45}$-*b*-(DMA$_{80}$-*s*-NAS$_{20}$)	7	73	15 500	17 100	1.11	16 500	PEO$_{45}$-*b*-(DMA$_{92}$-*s*-NAS$_{31}$)
3	PEO$_{45}$-*b*-(DMA$_{60}$-*s*-NAS$_{40}$)	5	80	15 700	17 800	1.14	15 100	PEO$_{45}$-*b*-(DMA$_{40}$-*s*-NAS$_{53}$)
4	PEO$_{45}$-*b*-(DMA$_{91}$-*s*-NAS$_{12}$)-*b*-NIPAM$_{80}$	16	70	21 100	24 300	1.16	19 700	PEO$_{45}$-*b*-(DMA$_{91}$-*s*-NAS$_{12}$)-*b*-NIPAM$_{57}$
5	PEO$_{45}$-*b*-(DMA$_{91}$-*s*-NAS$_{12}$)-*b*-NIPAM$_{120}$	24	73	23 600	29 700	1.26	23 200	PEO$_{45}$-*b*-(DMA$_{91}$-*s*-NAS$_{12}$)-*b*-NIPAM$_{88}$
6	PEO$_{45}$-*b*-(DMA$_{92}$-*s*-NAS$_{31}$)-*b*-NIPAM$_{80}$	16	69	24 400	28 000	1.14	22 500	PEO$_{45}$-*b*-(DMA$_{92}$-*s*-NAS$_{31}$)-*b*-NIPAM$_{53}$
7	PEO$_{45}$-*b*-(DMA$_{92}$-*s*-NAS$_{31}$)-*b*-NIPAM$_{120}$	24	74	28 600	35 200	1.23	26 800	PEO$_{45}$-*b*-(DMA$_{92}$-*s*-NAS$_{31}$)-*b*-NIPAM$_{91}$

[a] d*n*/d*c* = 0.081 was used to calculate the polymer molecular weight and molecular weight distribution. [b] Measured by ^{1}H NMR.

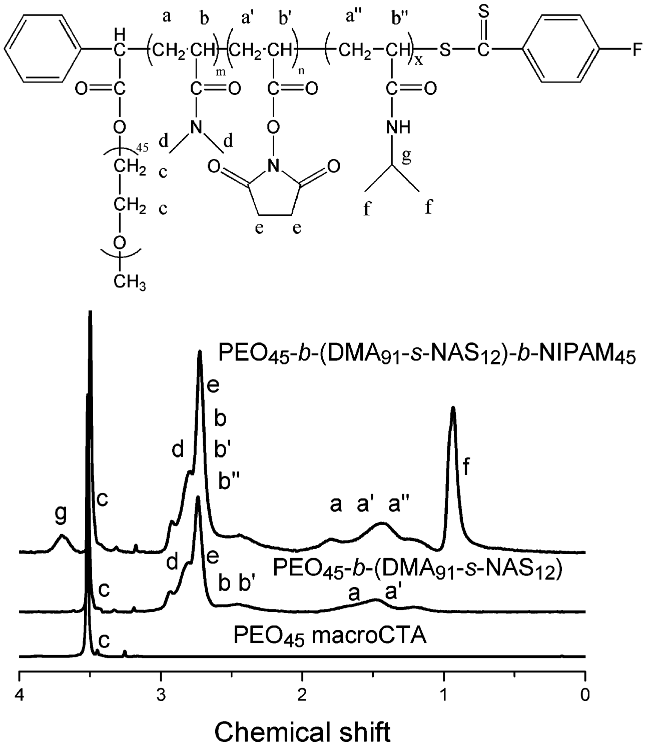

Figure 4. ^{1}H NMR spectra of the PEO$_{45}$-based macromolecular chain transfer agent (PEO$_{45}$-macro-CTA), PEO$_{45}$-*b*-(DMA$_{91}$-*s*-NAS$_{12}$) diblock copolymer, and PEO$_{45}$-*b*-(DMA$_{91}$-*s*-NAS$_{12}$)-*b*-NIPAM$_{45}$ triblock copolymers. PEO = poly(ethylene oxide); DMA = *N,N*-dimethylacrylamide; NAS = *N*-acryloxysuccinimide; NIPAM = *N*-isopropylacrylamide.

the RAFT polymerization of NIPAM (Scheme 2). All synthetic triblock copolymers have relatively low polydispersities (<1.3), and the chain transfer efficiency is high since there appear to be no low molecular weight side peaks which correspond to the PEO-*b*-(DMA-*s*-NAS) diblock macro-CTA (Figure 5).

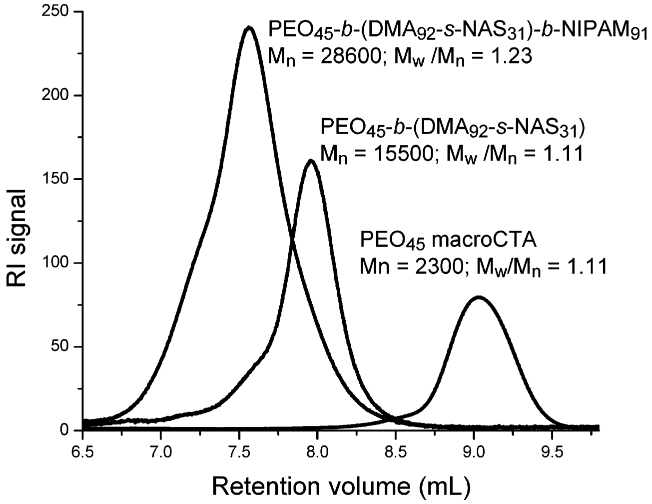

Figure 5. DMF SEC traces for (1) the PEO$_{45}$-based macromolecular chain transfer agent (PEO$_{45}$-macro-CTA), (2) the corresponding chain-extended PEO-*b*-(DMA-*s*-NAS) diblock copolymer, and (3) the PEO$_{45}$-*b*-(DMA-*s*-NAS)-*b*-NIPAM triblock copolymer. PEO = poly(ethylene oxide); DMA = *N,N*-dimethylacrylamide; NAS = *N*-acryloxysuccinimide; NIPAM = *N*-isopropylacrylamide.

Stability of the Triblock Copolymers in the Aqueous Solution. Although the NAS unit is less reactive with water as compared to primary amines,[52] it is not likely to be stable in aqueous solution for lengthy periods of time. For example, Charreyre et al.[52] recently reported that when D$_2$O was used as the deuterated solvent in the ^{1}H NMR experiment of DMA/NAS copolymers, even though the polymer solutions were prepared just before the analysis, a small signal at 2.75 ppm could be attributed to the CH$_2$ protons of NHS, indicating some hydrolysis of the activated ester groups. Thus, it was necessary for us to determine the hydrolytic stability of PEO-*b*-(DMA-*s*-NAS)-*b*-NIPAM triblock copolymers in aqueous solution. The polymer was dissolved in D$_2$O at 0.5% (w/w) concentration at room temperature, and ^{1}H NMR was used to monitor the appearance of the NHS. By comparing the integration areas of the PEO and NHS methylene proton resonances at 3.50 δ and 2.60 δ, respectively, the degree of hydrolysis can be calculated. From Figure 6, we can see that the PEO-*b*-(DMA-*s*-NAS)-*b*-NIPAM triblock copolymer is stable for at least several hours. After 7 h, only 0.3% of the NAS units had been hydrolyzed. Even after 12 days, 63% of the NAS units remain.

Micellization of the PEO-*b*-(DMA-*s*-NAS)-*b*-NIPAM Triblock Copolymers. The NAS monomer and its corresponding homopolymer are hydrophobic in nature. When NAS is copolymerized with DMA, a hydrophilic monomer, the copolymer will remain hydrophilic provided the NAS content is kept low. For example, PEO$_{45}$-*b*-(DMA$_{91}$-*s*-NAS$_{12}$) and PEO$_{45}$-*b*-(DMA$_{92}$-*s*-NAS$_{31}$) are sufficiently hydrophilic to dissolve molecularly in aqueous solution (as confirmed by ^{1}H NMR and dynamic light scattering). When the NAS content is increased further (for example, PEO$_{45}$-*b*-(DMA$_{40}$-*s*-NAS$_{53}$)), the diblock copolymer does not dissolve molecularly. Instead, a complex, micelle-like structure is formed. This behavior will be the subject of future studies; however, we focus here on the two hydrophilic diblock copolymers PEO$_{45}$-*b*-(DMA$_{91}$-*s*-NAS$_{12}$) and PEO$_{45}$-*b*-(DMA$_{92}$-*s*-NAS$_{31}$).

Figure 7 illustrates the dynamic light scattering (DLS) behavior of our NIPAM-based triblock copolymers prepared

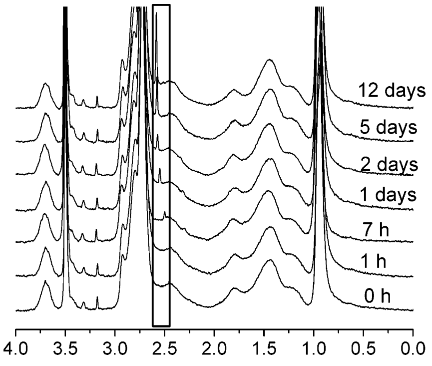

Figure 6. ^{1}H NMR spectra of PEO$_{45}$-*b*-(DMA$_{91}$-*s*-NAS$_{12}$)-*b*-PNIPAM$_{57}$ triblock copolymer in D$_2$O recorded at different times (25 °C). PEO = poly(ethylene oxide); DMA = *N*,*N*-dimethylacrylamide; NAS = *N*-acryloxysuccinimide; NIPAM = *N*-isopropylacrylamide. δ (ppm from TMS): 3.50 (CH_2−CH_2−O from PEO), 2.60 (CH_2−CH_2− from NHS). See Figure 4 for detailed proton assignment. Notice the appearance of the NHS signal at 2.60 ppm.

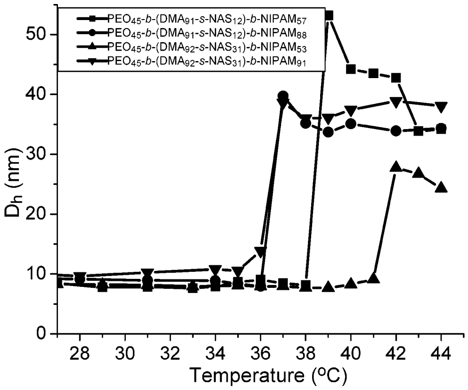

Figure 7. Hydrodynamic diameter vs temperature data for the four triblock copolymers in aqueous solution (0.5% (w/w) concentration). PEO = poly(ethylene oxide); DMA = *N*,*N*-dimethylacrylamide; NAS = *N*-acryloxysuccinimide; NIPAM = *N*-isopropylacrylamide.

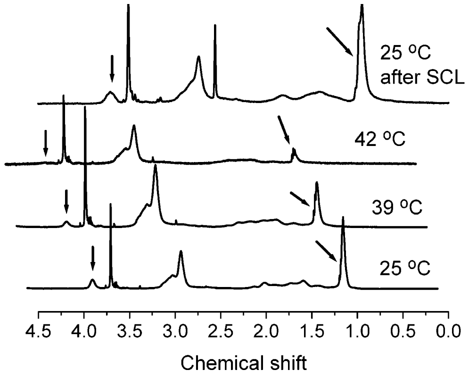

Figure 8. ^{1}H NMR spectra of the PEO$_{45}$-*b*-(DMA$_{92}$-*s*-NAS$_{31}$)-*b*-NIPAM$_{91}$ and the shell cross-linked derivative in D$_2$O at selected temperatures. PEO = poly(ethylene oxide); DMA = *N*,*N*-dimethylacrylamide; NAS = *N*-acryloxysuccinimide; NIPAM = *N*-isopropylacrylamide.

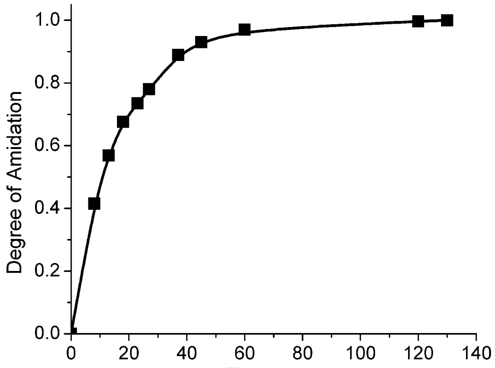

Figure 9. Degree of amidation vs time data for the reaction of PEO$_{45}$-*b*-(DMA$_{92}$-*s*-NAS$_{31}$)-*b*-NIPAM$_{91}$ with ethylenediamine at 45 °C. PEO = poly(ethylene oxide); DMA = *N*,*N*-dimethylacrylamide; NAS = *N*-acryloxysuccinimide; NIPAM = *N*-isopropylacrylamide.

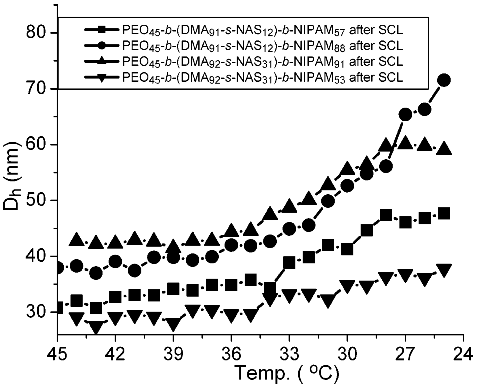

Figure 10. Variation of micelle hydrodynamic diameters with solution temperature after shell cross-linking. PEO = poly(ethylene oxide); DMA = *N*,*N*-dimethylacrylamide; NAS = *N*-acryloxysuccinimide; NIPAM = *N*-isopropylacrylamide.

from the above samples at a concentration of 0.50 wt %. At temperatures lower than the critical temperature, all four triblock copolymers are molecularly dissolved with hydrodynamic diameters ($\langle D_h \rangle$) of approximately 7−8 nm. By increasing the solution temperature above 37 °C, micellization occurs for the PEO$_{45}$-*b*-(DMA$_{92}$-*s*-NAS$_{31}$)-*b*-NIPAM$_{91}$ and PEO$_{45}$-*b*-(DMA$_{91}$-*s*-NAS$_{12}$)-*b*-NIPAM$_{88}$ triblock copolymers. However, PEO$_{45}$-*b*-(DMA$_{91}$-*s*-NAS$_{12}$)-*b*-NIPAM$_{57}$ and PEO$_{45}$-*b*-(DMA$_{92}$-*s*-NAS$_{31}$)-*b*-NIPAM$_{53}$ require higher temperatures (39 and 42 °C, respectively) to induce micellization. It seems that the micellization temperature is quite sensitive to the molecular weight of the NIPAM block. The higher the molecular weight of the NIPAM block, the lower the micellization temperature.

Although previous studies show that the LCST for PNIPAM is 32 °C, those polymers were made via conventional free radical polymerization.[64] Their molecular weights are higher and their molecular weight distributions are broader. Recent experiments by Stover et al.[65] also show that the LCST depends on the molecular weight of PNIPAM. As the molecular weight ($M_{n,NMR}$) increases from 2.8 to 26.5 kg/mol, the cloud point (50% T) drops from 43.0 to 33.3 °C and approaches the 31−32 °C range that is commonly reported for PNIPAM. This agrees with our current results which indicate that the micellization temperature ranges from 37 to 42 °C. Stover et al. also showed that, although the thermal transitions are quite sharp for higher molecular weight polymers, broadening occurs for lower molecular weight polymers, and the thermal transition for the 2.8 kg/mol sample occurs over a range of more than 10 °C. Solutions of our PEO$_{45}$-*b*-(DMA$_{92}$-*s*-NAS$_{31}$)-*b*-NIPAM$_{53}$ have an experimental micellization temperature of around 42 °C. However, there are some observable micelles of $\langle D_h \rangle \approx 35$ nm at 37 °C although their volume fraction is only 1.4%. The volume fraction of these micelles increases to 24% at 41 °C. Above 42 °C, micelle size decreases with increasing temperature. Such changes are not as obvious for polymers with longer NIPAM block since the thermal transitions are quite sharp for higher molecular weight polymers.[65]

Figure 8 shows the NMR spectra recorded for PEO$_{45}$-*b*-(DMA$_{92}$-*s*-NAS$_{31}$)-*b*-NIPAM$_{91}$ triblock copolymers at different

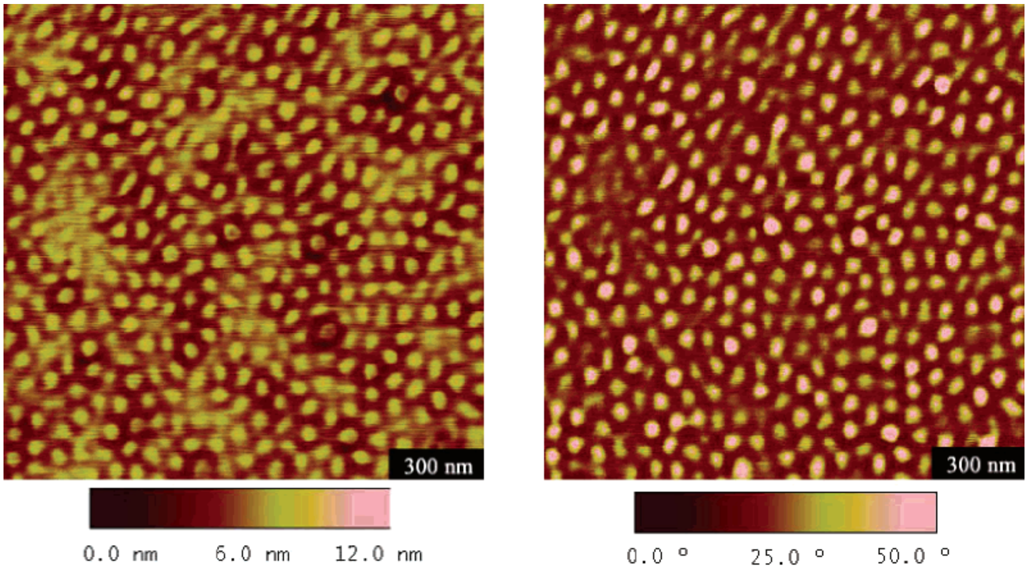

Figure 11. Tapping-mode AFM images of SCL micelles (left: height image; right: phase image). Samples were prepared by drop deposition (5 μL, 0.01% concentration) onto freshly cleaved mica and allowed to dry in air.

temperatures. At 25 °C, the copolymer chains are fully solvated, and signals expected for each block are visible. At 39 °C, DLS shows that micelles have been formed; although the peaks associated with the NIPAM block have become attenuated, they are still visible in the NMR spectra. Comparison of the NIPAM signal at δ 4.0 with the PEO signal at δ 3.7 indicates a 55% decrease in relative intensity for the former. This indicates that at 39 °C the NIPAM cores are still partially hydrophilic. Increasing the solution temperature to 42 °C causes the NIPAM signal to diminish since the NIPAM core becomes increasingly hydrophobic. This is also confirmed by DLS experiments: at 37 °C, the micelle polydispersity is relatively high (0.198), whereas at 39 °C the polydispersity decreases to 0.158. At 42 °C, micelles with uniform size distributions (polydispersity as low as 0.042) can be obtained.

Although all four triblock copolymers can form micelles, the polydispersities of the micelles vary with composition as might be predicted from the previous discussion. When the NIPAM block is shorter, the micelle polydispersity is higher. For example, the polydispersities for PEO_{45}-*b*-(DMA_{91}-*s*-NAS_{12})-*b*-$NIPAM_{57}$ and PEO_{45}-*b*-(DMA_{92}-*s*-NAS_{31})-*b*-$NIPAM_{53}$ at 44 °C are 0.214 and 0.143, respectively, while for PEO_{45}-*b*-(DMA_{91}-*s*-NAS_{12})-*b*-$NIPAM_{88}$ and PEO_{45}-*b*-(DMA_{92}-*s*-NAS_{31})-*b*-$NIPAM_{91}$, the micelle polydispersities at 44 °C are 0.081 and 0.042, respectively. Clearly, the hydrophobic block (NIPAM block) must be of sufficient length to allow micelles with uniform size distributions to be formed.

Shell Cross-Linking of the Triblock Copolymer Micelles. SCL micelles can be prepared by adding a bifunctional or multifunctional primary amine-containing compounds to the micellar solution. Here, ethylenediamine was used as a model compound to investigate the shell cross-linking of our micelles. Ethylenediamine can react with the NAS residues and hence lead to the cross-linking of the inner shell of the "onion"-like micelles.[41] Since the reaction of the NAS residues with ethylenediamine leads to the formation of NHS as a byproduct, the in-situ shell cross-linking can be monitored via ^{1}H NMR (see Supporting Information for the appropriate NMR spectrum). Figure 9 shows the degree of amidation vs time data. At 45 °C, the amidation reaction proceeds rapidly. After 30 min, the degree of amidation reaches 80%. From Figure 9, it can be seen that the maximum degree of amidation (>95%) is reached within 2 h. This is quite fast compared to other methods which may require several hours.[41] Even under ideal conditions, complete amidation does not lead to the 100% targeted degree of cross-linking. There are two reasons: first, only the reaction of ethylenediamine with the NAS residues on two different polymer chains can lead to *intermolecular* shell cross-linking. The reaction of ethylenediamine with NAS residues on the same polymer chain can only lead to *intramolecular* cross-linking, which does not produce SCL micelles. Second, some unavoidable hydrolysis of NAS in aqueous solution reduces the NAS units available for cross-linking, thus lowering the degree of cross-linking that is achieved.

After the cross-linking reaction, the resulting solution was allowed to cool to room temperature. If no shell cross-linking had occurred, dissociation into unimers would be expected. However, DLS experiments show that micelle size increases when the solution temperature is lowered below the LCST of the NIPAM block (Figure 10). Since the actual degree of cross-linking in our current system is not very high, we suggest that the NIPAM core becomes hydrophilic again below its LCST (as confirmed by ^{1}H NMR, Figure 8), causing the micelles to swell (Figure 10). The degree of swelling is highly dependent on the degree of cross-linking. For example, PEO_{45}-*b*-(DMA_{92}-*s*-NAS_{31})-*b*-$NIPAM_{91}$ and PEO_{45}-*b*-(DMA_{91}-*s*-NAS_{12})-*b*-$NIPAM_{88}$ have similar hydrophilic and hydrophobic block lengths and thus have similar micelle sizes. However, their NAS contents are different; thus, their degrees of cross-linking are different. PEO_{45}-*b*-(DMA_{92}-*s*-NAS_{31})-*b*-$NIPAM_{91}$ has a higher degree of shell cross-linking; this triblock swells 1.4 times its original size (from 42.2 to 60 nm) when the temperature is lowered from 45 to 25 °C. For PEO_{45}-*b*-(DMA_{91}-*s*-NAS_{12})-*b*-$NIPAM_{88}$, the extent of cross-linking is less; it swells 1.9 times its original size (from 38 to 71.5 nm). The same trend is also evident for PEO_{45}-*b*-(DMA_{91}-*s*-NAS_{12})-*b*-$NIPAM_{57}$ and PEO_{45}-*b*-(DMA_{92}-*s*-NAS_{31})-*b*-$NIPAM_{53}$. The above changes in size with temperature are fully reversible.

Figure 11 shows an AFM image of the SCL micelles prepared from PEO_{45}-*b*-(DMA_{92}-*s*-NAS_{31})-*b*-$NIPAM_{91}$. It can be seen that the micelles are relatively uniform in diameter, ~75 nm, slightly larger than in aqueous solution at 25 °C (60 nm). AFM analysis also shows that the height of the SCL micelles is only 8−9 nm (Figure 11, height image), which is significantly less than the micelles diameter. All of these indicate some flattening of the partially swollen (loose) SCL micelles on the AFM substrate as reported by Wooley et al.[8,66,67]

Conclusions

A PEO-based macro-CTA was successfully employed to control the RAFT polymerization of DMA and the statistical copolymerization of DMA with NAS. The resulting diblock copolymers were then used to mediate the RAFT polymerization of NIPAM. Well-defined PEO-*b*-(DMA-*s*-NAS)-*b*-NIPAM triblock copolymers were obtained. These thermally responsive triblock copolymers dissolve molecularly in aqueous solution at 20 °C and self-assemble to form micelles when the temperature is raised above the LCST of the NIPAM block. The middle layer of the micelles (DMA-*s*-NAS block) can be easily cross-linked with a difunctional primary amine-containing compound. These SCL micelles swell when the solution temperature is lower than the LCST of the NIPAM block. The utility of NAS as the active monomer is that a variety of comonomers can be envisioned for preparation of SCL micelles providing that they can copolymerize with NAS.

Acknowledgment. We gratefully acknowledge the financial support provided by the Department of Energy (DE-FC26-01BC15317) and the MRSEC program of the National Science Foundation (DMR-0213883). We thank Professor Steven P. Armes for helpful insight into the behavior of PEO-based shell cross-linked micelles. We thank Dr. Sarah E. Morgan and Dr. Jun Li for their assistance in AFM analysis.

Supporting Information Available: ^{1}H NMR spectra recorded during shell cross-linking of PEO$_{45}$-*b*-(DMA$_{92}$-*s*-NAS$_{31}$)-*b*-NIPAM$_{91}$ formed micelles with ethylenediamine. This material is available free of charge via the Internet at http://pubs.acs.org.

References and Notes

(1) Thurmond, K. B.; Kowalewski, T.; Wooley, K. L. *J. Am. Chem. Soc.* **1996**, *118*, 7239−7240.

(2) Wooley, K. L. *J. Polym. Sci., Part A*: *Polym. Chem.* **2000**, *38*, 1397−1407.

(3) Thurmond, K. B.; Kowalewski, T.; Wooley, K. L. *J. Am. Chem. Soc.* **1997**, *119*, 6656−6665.

(4) Huang, H.; Remsen, E. E.; Wooley, K. L. *Chem. Commun.* **1998**, 1415−1416.

(5) Huang, H.; Remsen, E. E.; Kowalewski, T.; Wooley, K. L. *J. Am. Chem. Soc.* **1999**, *121*, 3805−3806.

(6) Ma, Q.; Wooley, K. L. *J. Polym. Sci., Part A*: *Polym. Chem.* **2000**, *38*, 4805−4820.

(7) Becker, M. L.; Remsen, E. E.; Wooley. K. L. *J. Polym. Sci., Part A*: *Polym. Chem.* **2001**, *39*, 4152−4166.

(8) Ma, Q.; Remsen, E. E.; Kowalewski, T.; Wooley, K. L. *J. Am. Chem. Soc.* **2001**, *123*, 4627−4628.

(9) Sanji, T.; Nakatsuka, Y.; Kitayama, F.; Sakurai, H. *Chem. Commun.* **1999**, 2201−2202.

(10) Sanji, T.; Nakatsuka, Y.; Ohnishi, S.; Sakurai, H. *Macromolecules* **2000**, *33*, 8524−8526.

(11) Underhill, R. S.; Liu, G. *Chem. Mater.* **2000**, *12*, 2082−2091.

(12) Fujii, S.; Cai, Y.; Weaver, J. V. M.; Armes, S. P. *J. Am. Chem. Soc.* **2005**, *127*, 7304−7305.

(13) Butun, V.; Wang, X.-S.; de Paz Banez, M. V.; Robinson, K. L.; Billingham, N. C.; Armes, S. P. *Macromolecules* **2000**, *33*, 1−3.

(14) Liu, S.; Armes, S. P. *J. Am. Chem. Soc.* **2001**, *123*, 9910−9911.

(15) Butun, V.; Billingham, N. C.; Armes, S. P. *J. Am. Chem. Soc.* **1998**, *120*, 12135−12136.

(16) Butun, V.; Lowe, A. B.; Billingham, N. C.; Armes, S. P. *J. Am. Chem. Soc.* **1999**, *121*, 4288−4289.

(17) Pilon, L. N.; Armes, S. P.; Findlay, P.; Rannard, S. P. *Langmuir* **2005**, *21*, 3808−3813.

(18) Huang, H.; Kowalewski, T.; Remsen, E. E.; Gertzmann, R.; Wooley, K. L. *J. Am. Chem. Soc.* **1997**, *119*, 11653−11659.

(19) Zhang, Q.; Remsen, E. E.; Wooley, K. L. *J. Am. Chem. Soc.* **2000**, *122*, 3642−3651.

(20) Liu, S.; Weaver, J. V. M.; Save, M.; Armes, S. P. *Langmuir* **2002**, *18*, 8350−8357.

(21) Stewart, S.; Liu, G. *J. Chem. Mater.* **1999**, *11*, 1048−1054.

(22) Weaver, J. V. M.; Tang, Y. Q.; Liu, S.; Iddon, P. D.; Grigg, R.; Armes, S. P.; Billingham, N. C.; Hunter, R.; Rannard, S. P. *Angew. Chem.* **2004**, *43*, 1389−1392.

(23) Hawker, C. J.; Bosman, A. W.; Harth, E. *Chem. Rev.* **2001**, *101*, 3661−3688.

(24) Matyjaszewski, K.; Xia, J. *Chem. Rev.* **2001**, *101*, 2921−2990.

(25) Moad, G.; Rizzardo. E.; Thang, S. H. *Aust. J. Chem.* **2005**, *58*, 379−410.

(26) Kamigaito, M.; Ando, T.; Sawamoto, M. *Chem. Rev.* **2001**, *101*, 3689−3745.

(27) Rizzardo, E.; Chiefari, J.; Chong, Y. K.; Ercole, F.; Krstina, J.; Jeffery, J.; Le T. P. T.; Mayadunne, R. T. A.; Meijs, G. F.; Moad, C. L.; Moad, G.; Thang, S. H. *Macromol. Symp.* **1999**, *143*, 291−307.

(28) Rizzardo, E.; Chiefari, J.; Mayadunne, R. T. A.; Moad, G.; Thang, S. H. *ACS Symp. Ser.* **2000**, *768*, 278−296.

(29) Matyjaszewski, K., Davis, T. P., Eds.; *Handbook of Radical Polymerization*; John Wiley & Sons: Hoboken, NJ, 2002.

(30) Moad, G.; Chiefari, J.; Krstina, J.; Postma, A.; Madayunne, R. T. A.; Rizzardo, E.; Thang, S. H. *Polym. Int.* **2000**, *49*, 993−1001.

(31) McCormick, C. L.; Lowe, A. B. *Acc. Chem. Res.* **2004**, *37*, 312−325.

(32) Sumerlin, B. S.; Donovan, M. S.; Mitsukami, Y.; Lowe, A. B.; McCormick, C. L. *Macromolecules* **2001**, *34*, 6561−6564.

(33) Sumerlin, B. S.; Lowe, A. B.; Thomas, D. B.; McCormick, C. L. *Macromolecules* **2003**, *36*, 5982−5987.

(34) Vasilieva, Y. A.; Thomas, D. B.; Scales, C. W.; McCormick, C. L. *Macromolecules* **2004**, *37*, 2728−2737.

(35) Donovan, M. S.; Lowe, A. B.; Sanford, T. A.; McCormick, C. L. *J. Polym. Sci., Part A*: *Polym. Chem.* **2003**, *41*, 1262−1281.

(36) Donovan, M. S.; Sumerlin, B. S.; Lowe, A. B.; McCormick, C. L. *Macromolecules* **2002**, *35*, 8663−8666.

(37) Donovan, M. S.; Sanford, T. A.; Lowe, A. B.; Sumerlin, B. S.; Mitsukami, Y.; McCormick, C. L. *Macromolecules* **2002**, *35*, 4570−4572.

(38) Thomas, D. B.; Sumerlin, B. S.; Lowe, A. B.; McCormick, C. L. *Macromolecules* **2003**, *36*, 1436−1439.

(39) Convertine, A. J.; Ayres, N.; Scales, C. W.; Lowe, A. B.; McCormick, C. L. *Biomacromolecules* **2004**, *5*, 1177−1180.

(40) Pollak, A.; Blumenfeld, H.; Wax, M.; Baughn, R. L.; Whitesides, G. M. *J. Am. Chem. Soc.* **1980**, *102*, 6324−6336.

(41) Liu, S.; Weaver, J. V. M.; Tang, Y.; Billingham, N. C.; Armes, S. P.; Tribe, K. *Macromolecules* **2002**, *35*, 6121−6131.

(42) Chong, Y. K.; Le, T. P. T.; Moad, G.; Rizzardo, E.; Thang, S. H. *Macromolecules* **1999**, *32*, 2071−2074.

(43) Perrier, S.; Takolpuckdee, P.; Westwood, J.; Lewis, D. M.; *Macromolecules* **2004**, *37*, 2709−2717.

(44) Donovan, M. S.; Lowe, A. B.; Sumerlin, B. S.; McCormick, C. L. *Macromolecules* **2002**, *35*, 4123−4132.

(45) Benaglia, M.; Rizzardo, E.; Alberti, A.; Guerra, M. *Macromolecules* **2005**, *38*, 3129−3140.

(46) Mayadunne, R. T. A.; Rizzardo, E.; Chiefari, J.; Chong, Y. K.; Moad, G.; Thang, S. H. *Macromolecules* **1999**, *32*, 6977−6980.

(47) Chong, Y. K.; Krstina, J.; Le, T. P. T.; Moad, G.; Postma, A.; Rizzardo, E.; Thang, S. H. *Macromolecules* **2003**, *36*, 2256−2272.

(48) Farmer, S. C.; Patten, T. E. *J. Polym. Sci., Polym. Chem.* **2002**, *40*, 555−563.

(49) Perrier, S.; Barner-Kowollik, C.; Quinn, J. F.; Vana, P.; Davis, T. P. *Macromolecules* **2002**, *35*, 8300−8306.

(50) Rizzardo, E.; Chiefari, J.; Mayadunne, R.; Moad, G.; Thang, S. *Macromol. Symp.* **2001**, *174*, 209−212.

(51) Baum, M.; Brittain, W. J. *Macromolecules* **2002**, *35*, 610−615.

(52) Relogio, P.; Charreyre, M.-T.; Farinha, J. P. S.; Martinho, J. G. M.; Pichot, C. *Polymer* **2004**, *45*, 8639−8649.

(53) Favier, A.; D'Agosto, F.; Charreyre, M.-T.; Pichot, C. *Polymer* **2004**, *45*, 7821−7830.

(54) Matyjaszewski, K., Ed. *Advances in Controlled/Living Radical Polymerization*; ACS Symposium Series Vol. 854; American Chemistry Society: Washington, DC, 2003; pp 603−618.

(55) de Lambert, B.; Chaix, C.; Charreyrex, M.-T.; Laurent, A.; Aigoui, A.; Perrin-Rubens, A.; Pichot, C. *Bioconjugate Chem.* **2005**, *16*, 265−274.

(56) Vosloo, J. J.; Tonge, M. P.; Fellows, C. M.; D'Agosto, F.; Sanderson, R. D.; Gilbert, R. G. *Macromolecules* **2004**, *37*, 2371−2382.

(57) Eeckman, F.; MoNs, A. J.; Amighi, K. *Int. J. Pharm.* **2004**, *273*, 109−119.

(58) Eeckman, F.; MoNs, A. J.; Amighi, K. *Eur. Polym. J.* **2004**, *40*, 873−881.

(59) Dube, D.; Francis, M.; Lerous, J. C.; Winnik, F. M. *Bioconjugate Chem.* **2002**, *13*, 685−692.

(60) Ganachaud, F.; Monteiro, M. J.; Gilbert, R. G.; Dourges, M.-A.; Thang, S. H.; Rizzardo, E. *Macromolecules* **2000**, *33*, 6738−6745.

(61) Schilli, C.; Lanzendoerfer, M. G.; Mueller, A. H. E. *Macromolecules* **2002**, *35*, 6819−6827.

(62) Ray, B.; Isobe, Y.; Morioka, K.; Habaue, S.; Okamoto, Y.; Kamigaito, M.; Sawamoto, M. *Macromolecules* **2003**, *36*, 543−545.

(63) Ray, B.; Isobe, Y.; Matsumoto, K.; Habaue, S.; Okamoto, Y.; Kamigaito, M.; Sawamoto, M. *Macromolecules* **2004**, *37*, 1702−1710.

(64) Schild. H. G. *Prog. Polym. Sci.* **1992**, *17*, 163−249.

(65) Xia, Y.; Yin, X.; Burke, N. A. D.; Stover, H. D. H. *Macromolecules* **2005**, *38*, 5937−5943.

(66) Joralemon, M. J.; Smith, N. L.; Holowka, D.; Baird, B.; Wooley, K. L. *Bioconjugate Chem.* **2005**, *16*, 1246−1256.

(67) Pan, D.; Turner, J. L.; Wooley, K. L. *Macromolecules* **2004**, *37*, 7109−7115.

(68) Turner, J. L.; Wooley, K. L. *Nano Lett.* **2004**, *4*, 683−688.

MA052116R